Nanocomposites of linseed mucilage and k-carrageenan loaded with *Achyrocline satureioides* nanoemulsion: a gradual-release candidate of antimicrobials for the treatment of bovine mastitis

Gabriela Tasso Pinheiro Machado, Roberto Gabriel Ferreira, Maria Beatriz Veleirinho, Luciana Aparecida Honorato, Roberta de Oliveira Ramos, Marcos Antônio Segatto Silva and Shirley Kuhnen

SUPPLEMENTARY FILE

Material and methods

Table S1. Nanocomposites (NCs) developed with different proportions of k-carrageenan and linseed mucilage (w/w).

Composition (w/w)	k-carrageenan	NC-9:1	NC-8:2	NC-7:3	NC-6:4	NC-5:5	Linseed mucilage
k-carrageenan (g)[1]	10	5	5	5	5	5	-
k-carrageenan (g)[2]	-	4	3	2	1	-	L
Linseed mucilage (g)	-	1	2	3	4	5	10

(1) carrageenan prepared in the macela nanoemulsion (2.5 mg/mL of the macela extract); (2) carrageenan prepared in distilled water.

Fourier-transform infrared spectroscopy (FTIR)

Infrared spectroscopy (FTIR) was performed on a PerkinElmer Spectrum One fitted with a universal ATR sampling accessory. IR spectra were recorded in the frequency range 4000-400 cm^{-1} using 16 scans per sample cycle. Data were analyzed using a Spectrum software (PerkinElmer Spectrum™ 10).

HPLC analysis

The samples were analyzed on a Thermo Scientific UltiMate 3000 RS Dual HPLC System (Thermo Fisher Scientific, San Jose, CA) using a C18 reverse phase column (4.6

x 150 mm; 5 µm; 120Å; AcclaimTM120, Thermo Scientific ©) at 25° C, operating at 240, 270, 320 and 375 nm. The mobile phase consisted of Milli-Q® water acidified to pH 2.3 (A) and methanol (B) eluted at 1.0 mL min flow^{-1} using the following gradient program: 0-5 min, 90% A; 5-25 min, 30% A; 25-37 min, 90% A. The identification of 3-O-methylquercetin (3-O-MQ) was performed by comparison with the retention times of commercial standards (Sigma-Aldrich). The identification of achyrobichalcone (ACB) was carried out at the Galenic Development Laboratory (UFRGS) according to the methodology described by Bianchi *et al*. (2019) and Carini *et al.* (2013). Quantification was based on the integration of the peak areas through the quercetin calibration curve (Sigma-Aldrich; Q4951) (concentration range of 0.97-1000 µg mL^{-1}, $r^2 > 0.999$, y = 0.168x) (Pinheiro Machado *et al.* 2020). The detection limit (DL) was of 0.19 µg mL^{-1} whereas the quantification limit (QL) was of 0.63 µg mL^{-1}. For the standard deviation of the response (σ), the *y*-intercepts obtained from three calibration curves were considered, and for S, the slope of the mean calibration curve was considered.

Broth microdilution method for minimum inhibitory concentration (MIC) test

An aliquot of supernatant of NCs (100 µL) was added to 100 µL of Muller Hinton broth (MH). The tested concentrations corresponded to the concentration of macela extract in the NCS (1250-10 µg/mL). The initial population density of the inoculum was standardized through turbidity control equivalent to a standard 0.5 McFarland solution (1.5x10^7 to 10^8 CFU mL^{-1}). After dilution, 10 µL of the bacterial inoculum standard corresponding to 1.5x10^5 CFU mL^{-1} was added to microplate wells and incubated at 35ºC for 20 h. For comparison, the supernatant of UNCs was tested at the same concentrations. The percentage of bacterial growth inhibition was determined by reading the absorbance at 625 nm using a microplate reader (EL808, Bio-Tek Instruments, Inc., Winooski, USA) and the following formula: BI (%) = [1 – (AT/AI) X 100], where BI is bacterial growth inhibition, AT is the mean absorbance of the NCs concentrations - tested with inoculum subtracted from the absorbance value of the same NCs concentrations without the

addition of inoculum, and AI is the mean absorbance of the control microbial growth.

The minimum inhibitory concentration (MIC) was determined as the concentrations that

showed no visible growth, which was confirmed by the addition of 50 µL of resazurin (7-

hydroxy-3H-phenoxazin-3-one 10-oxide) (100 µg mL-1). In this case, metabolically

active cells can reduce blue-stained resazurin to pink-stained resorufin (Sarker *et al.*

2007).

Cytotoxicity of unloaded composites (UNCs) on the MAC-T cell line

Bovine epithelial cells of the MAC-T (mammary alveolar cells -T) lineage from the Cell

Bank of Rio de Janeiro (BCRJ) were maintained in the culture. Briefly, MAC-T cells

were cultivated in Dulbecco's Modified Eagle's Medium (DMEM) and supplemented

with 100 µg/mL of penicillin, 100 µg/mL of streptomycin, 20% (v/v) heat-inactivated

fetal bovine serum (FBS, Gibco, CA, USA), 4 mM L-glutamine (Synth), 4.5 g/L glucose

(Sigma-Aldrich, St. Louis, MO, USA), 1 mM of sodium pyruvate (Sigma-Aldrich, St.

Louis, MO, USA), 1.5 g/L sodium bicarbonate (VetecTM Sigma-Aldrich, St. Louis, MO,

USA), 5 µg/mL insulin (Sigma- Aldrich, St. Louis, MO, USA), and 1 µg/mL

hydrocortisone (Sigma –Aldrich, St. Louis, MO, USA) at 37° C and 5% CO_2 in a

humidified incubator. The medium was changed every 48 h. When the cells reached 70%

of confluence, they were treated with 0.25% trypsin in 1 mM EDTA to prepare the

cellular suspension (10^5 cells/mL). The suspension was transferred to a 96-well

microplate (100 µL/well), followed by incubation (24 h) in culture conditions for

adherence. Simultaneously, the UNCs were placed in DMEM medium (extraction

medium) and kept for 24 h under the same conditions of cell culture. After 24 h (cell

adhesion period), the culture medium in the plates was replaced by the extraction

medium, and the cells were cultured for further 24 h. Cytotoxicity was determined based

on the MTT ((3-(4,5-dimethylthiazol-2-yl)-2,5-diphenyltetrazolium bromide; 0.5

mg/mL) method. In this assay, it is quantified as the MTT present in the medium was

reduced by cellular metabolic activity linked to NADH and NADHP, forming crystals of

formazan blue color (Mosmann 1983). The formed formazan was dissolved with dimethyl sulfoxide (DMSO) to give a purple color with characteristic absorption at 540 nm. Intensity of purple color is directly proportional to the number of viable cells, thus indicating cell viability. Cells cultivated in untreated DMEM were considered to be 100% viable. The experiments were performed in triplicate.

Results

Characterization of nanocomposites

Figure S1. Macroscopic image of nanocomposites (NCs) in the proportions of k-carrageenan/linseed mucilage NC-5:5, NC-7:3 and NC-8:2 (w/w) loaded with 1.25 mg of macela extract/g of gel.


UV-VIS analysis

The differences between the three materials were found only at the initial times of 2 and 4 h, in which NC-7:3 and NC-8:2 showed less dissolution (Figure S2). Such differences are probably due to the lower dissolution of NCs with higher k-carrageenan content (Table 1). A previous study related the high water retention capacity of k-carrageenan to the release of bioactive compounds by disintegration, instead of swelling (Tapia *et al.* 2004). The greater initial and sustained dissolution over time presented by NC-5:5 may be more interesting for microbial control in the context of the treatment of

bovine mastitis in the dry period, because the initial phase of this period has been the most critical for microbial infections (Sordillo 2016).

Figure S2. Turbidity profile determined via UV-VIS (300 nm) as an estimate of the release of macela-nanoemulsion loaded in nanocomposites (NCs) containing the proportions of k-carrageenan and linseed mucilage 8:2, 7:3 and 5:5 (w/w), respectively over 72 h. The results are expressed as mean ± SD.
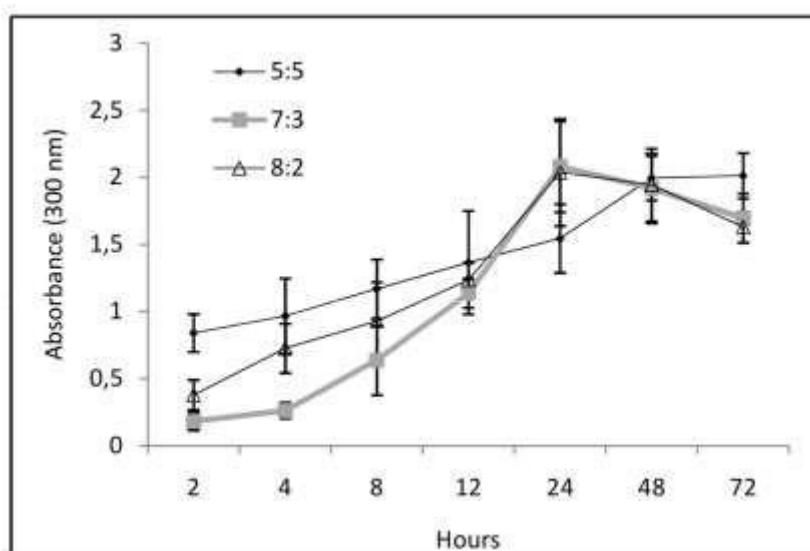
Fourier-transform infrared spectroscopy (FTIR)

Figure S3a shows the spectral profiles of the macela-nanoemulsion, and its components, i.e., linseed oil and macela extract. Since phenolic compounds are predominant in the macela extract (Pinheiro Machado *et al.* 2020, Retta *et al.* 2012), characteristic bands of these compounds - e.g., ~ 3272 cm^{-1}, (O-H phenol), 2926-2854 cm^{-1} (CH stretch) and 1604-1400 cm^{-1} (aromatic C = C) - could be identified in the corresponding spectrum (Figure S3a). In the linseed oil, one could find the characteristic bands of unsaturated fatty acids, such as 3010-2854 cm^{-1} (C-H unsaturated and aliphatic compounds, respectively), ~ 1744 cm^{-1} (C = C stretch) and ~ 722 cm^{-1} (CH$_2$ long-chain bands) (Figure S3a). In the spectrum corresponding to the macela-nanoemulsion, one can also see bands ~ 2924 cm^{-1}, ~ 2850 cm^{-1}, ~ 1744 cm^{-1}, which can be attributed to the

linseed oil and the macela extract (Figure S3a). Figure S3b shows the FTIR spectra representative of lyophilized NC-5:5, NC-7:3 and NC-8:2 and of the UNCs (unloaded composites; UNC-5:5 UNC-7:3 and UNC-8:2). There are no significant differences when comparing the spectra of the UNCs and NCs, i.e., the different concentrations of k-carrageenan and linseed mucilage did not significantly interfere in FTIR characterization.

Figure S3. (a) FTIR spectra of the macela-nanoemulsion, lyophilized macela extract and linseed oil, components of the nanoemulsion incorporated in the developed NCs. **(b)** FTIR spectra of NC-5:5, NC-7:3 and NC-8:2 loaded with the macela-nanoemulsion and the UNCs (unloaded composites UN-5:5, UN-7:3 and UN-8:2).
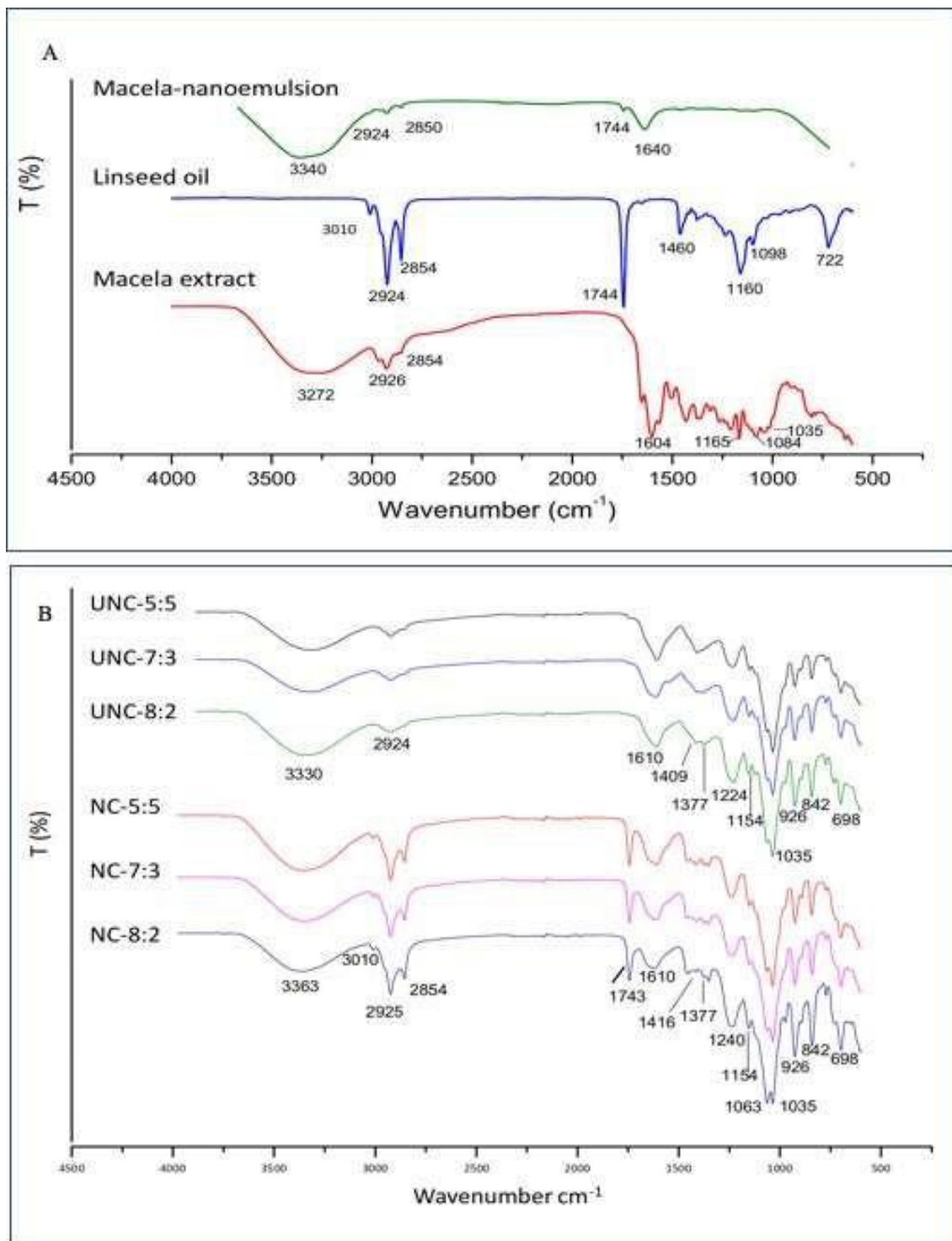
Table S2 shows FTIR of k-carrageenan, linseed mucilage and linseed polysaccharides, as reported in the literature.

Table S2. List of the characteristic FTIR bands found in the literature and comparison with the bands found in this study.

Bands (cm^{-1})	Group Vibration Modes	UNCs (cm^{-1})	NCs (cm^{-1})	Reference
3340	O-H, (glycerol bound and integrated with carrageenan in the formation of the hydrogel)	3330	3363	Vanegas et al. 2019
3294	O-H of polysaccharides			Mujtaba et al. 2019
3450	O-H			Haseeb et al. 2019
2924	C-H stretch of polysaccharides	2924	3010 (C-H) 2925	Mujtaba et al. 219
2900	C-H		2854 and 1743 (C=C)	Haseeb et al. 2019
1640 and 1420	deprotonated carboxylic groups (COO$^-$)	1610	1610	Haseeb et al. 2019
1643	C = O stretch of the protein			Mujtaba et al. 2019
1417	CH group in-plane vibrations	1409	1416	Mujtaba et al. 2019
1422 and 1226	stretch of the ester-sulfate bonds	1377	1377	Vanegas et al. 2019
1226	sulfate ester	1224	1240	Vanegas et al. 2019
1200 to 1000	C-O-C glycosidic bond and C-O-H stretching vibrations of the side groups of the polysaccharide			Haseeb et al. 2019
1158	CO of the 3,6-anhydro-1-galactopyranose ring (displaced by 1034 cm^{-1})	1154	1154	Vanegas et al. 2019
1033	glycosidic bond of hemicellulosic polysaccharides	1035	1063 1035	Mujtaba et al. 2019
912	K-carrageenan CO a, indicating 3,6-anhydro-d-galactose group	926	926	Vanegas et al. 2019
844	CO-SO$_4$ on the C4 carbon of d-galactose-4-sulfate	842	842	Vanegas et al. 2019
697	bending of the galactose ring	698	698	

When evaluating the spectra of both UNCs and NCs, one can detect the various characteristic bands previously reported in the literature (Table S1). When relating UNCs and NCs, it was found that, in the presence of the nanoemulsion, some characteristic bands seen in UNCs were maintained; moreover, there was a slight displacement of the O-H band, from ~ 3330 to 3363 cm^{-1} (C = O), which possibly occurred owing to the presence of hydrogen bonds when adding the nanoemulsion (Muhammad *et al.* 2019). Also, on the spectra referring to the NCs, bands appear at ~ 3010 cm^{-1}, ~ 2925 cm^{-1} (intensified), ~ 2854 cm^{-1} and ~ 1744 cm^{-1}, all of which are attributed to the presence of linseed oil, especially the first and the last, while the others are attributed to the macela extract, whose bands were already discussed in their isolated spectra (Figure S3a). As the analysis of the FTIR spectral profiles of the materials developed did not reveal a clear difference between them, except for the incorporation of the macela nanoemulsion (Table S1), multivariate analysis was used in order to carry out an exploratory and discriminatory analysis of the NCs and UNCs aiming at detecting possible differences not perceptible to the naked eye. The results of these analyzes reinforced the hypothesis that there is only physical interaction between the nanoemulsion and the polymers, i.e., k-carrageenan and linseed mucilage, components of the developed nanocomposites (data not shown). This finding confirms the addition of the nanoemulsion in the NCs by FTIR. Chemical interaction between the components could not be evidenced by the technique used; therefore, one can suggest a possible physical interaction between them, although techniques should be applied in the future to confirm this result.

Figure S4. (A) Bacterial activity after exposure to different concentrations of NC-5:5 (w/w), showing a MIC of 312 µg/mL, and (B) bacterial activity after exposure to different concentrations of NCs-7:3 and 8:2 (w/w), showing a MIC of 625 µg/mL. The pink color indicates growth and blue means inhibition of growth by resazurin metabolization.
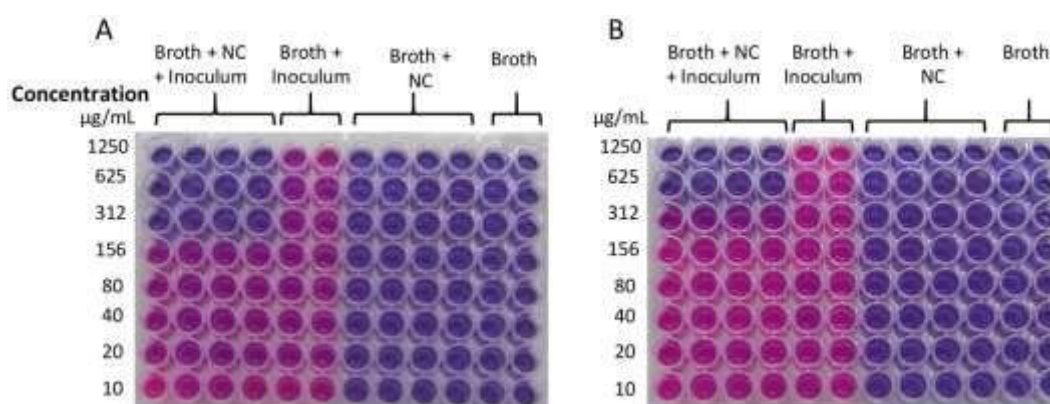
REFERENCES

Bianchi SE, Kaiser S, Pittol V, Doneda E, De Souza KCB, Bassani VL (2019) Semi-preparative isolation and purification of phenolic compounds from *Achyrocline satureioides* (Lam) DC by high-performance counter-current chromatography. *Phytochemical Analysis* **30**(2), 182-192.

Carini JP, Kaiser S, Ortega GG, Bassani VL (2013) Development, optimisation and validation of a stability-indicating HPLC method of achyrobichalcone quantification using experimental designs. *Phytochemical Analysis* **24**(3), 193-200.

Haseeb MT, Hussain MA, Yuk SH, Bashir S, Nauman M (2016) Polysaccharides based superabsorbent hydrogel from Linseed: Dynamic swelling, stimuli responsive on–off switching and drug release. *Carbohydrate polymers* **136**, 750-756.

Mosmann T (1983) Rapid colorimetric assay for cellular growth and survival: application to proliferation and cytotoxicity assays. *Journal of immunological methods* **65**(1-2), 55-63.

Muhamad II, Lazim NAM, Selvakumaran S (2019) Natural polysaccharide-based composites for drug delivery and biomedical applications. In *Natural Polysaccharides in Drug Delivery and Biomedical Applications.* Academic Press, pp. 419-440.

Mujtaba M, Akyuz L, Koc B, Kaya M, Ilk S, Cansaran-Duman D, Martinez AS, Cakmak, YS, Labidi J, Boufi S. (2019) Novel, multifunctional mucilage composite films incorporated with cellulose nanofibers. *Food Hydrocolloids* **89**, 20-28.

Pinheiro Machado GTP, Veleirinho MB, Honorato LA, Kuhnen S (2020) Formulation and evaluation of anti-MRSA nanoemulsion loaded with Achyrocline satureioides: a new sustainable strategy for the bovine mastitis. *Nano Express* **1**(3), 030004.

Sarker SD, Nahar L, Kumarasamy Y (2007) Microtitre plate-based antibacterial assay incorporating resazurin as an indicator of cell growth, and its application in the in vitro antibacterial screening of phytochemicals. *Methods* **42**(4), 321-324.

Sordillo LM (2016) Physiology of the mammary gland at dry-off: What do we really know?. *Tieraerztliche Umschau* **71**(3), 51.

Tapia C, Escobar Z, Costa E, Sapag-Hagar J, Valenzuela F, Basualto C, Gai MN, Yazdani-Pedram M (2004) Comparative studies on polyelectrolyte complexes and mixtures of chitosan–alginate and chitosan–carrageenan as prolonged diltiazem clorhydrate release systems. *European Journal of Pharmaceutics and Biopharmaceutics* **57**(1), 65-75.

Vanegas JS, Torres GR, Campos BB (2019) Characterization of a κ-Carrageenan Hydrogel and its Evaluation as a Coating Material for Fertilizers. *Journal of Polymers and Environment* **27**, 774–783.